Efficient dipole-dipole coupling of Mott-Wannier and Frenkel excitons in (Ga,In)N quantum well/polyfluorene semiconductor heterostructures

G. Itskos,[1,*] G. Heliotis,[1] P. G. Lagoudakis,[2] J. Lupton,[2] N. P. Barradas,[3] E. Alves,[3] S. Pereira,[4] I. M. Watson,[5] M. D. Dawson,[5] J. Feldmann,[2] R. Murray,[1] and D. D. C. Bradley[1]

[1]*Blackett Laboratory, Imperial College London, Prince Consort Road, SW7 2AZ, London, United Kingdom*

[2]*Department of Physics, Ludwig-Maximilians-Universität, 80799 Munich, Germany*

[3]*Instituto Technológico e Nuclear, E.N. 10, Apartado 21, 2658-953 Sacavém, Portugal*

[4]*CICECO, Departamento de Física, Universidade de Aveiro, 3810-193 Aveiro, Portugal*

[5]*Institute of Photonics, SUPA, University of Strathclyde, 106 Rottenrow, G4 0NW, Glasgow, United Kingdom*

(Received 25 January 2007; revised manuscript received 14 May 2007; published 31 July 2007)

We investigate interactions between Mott-Wannier (MW) and Frenkel excitons in a family of hybrid structures consisting of thin organic (polyfluorene) films placed in close proximity (systematically adjusted by GaN cap layer thickness) to single inorganic [(Ga,In)N/GaN] quantum wells (QWs). Characterization of the QW structures using Rutherford backscattering spectrometry and atomic force microscopy allows direct measurement of the thickness and the morphology of the GaN cap layers. Time-resolved photoluminescence experiments in the 8–75 K temperature range confirm our earlier demonstration that nonradiative energy transfer can occur between inorganic and organic semiconductors. We assign the transfer mechanism to resonant Förster (dipole-dipole) coupling between MW exciton energy donors and Frenkel exciton energy acceptors and at 15 K we find transfer efficiencies of up to 43%. The dependence of the energy transfer rate on the distance R between the inorganic QW donor dipole and organic film acceptor dipole indicates that a plane-plane interaction, characterized by a $1/R^2$ variation, best describes the situation found in our structures.

DOI: 10.1103/PhysRevB.76.035344 PACS number(s): 78.67.Pt, 71.35.Gg, 78.66.Qn

I. INTRODUCTION

Förster resonant energy transfer[1] (FRET) from a semiconductor quantum well (QW) energy donor to an organic energy acceptor material has been predicted to become an efficient process when the two materials are placed in close proximity (interaction distance, $R \approx$ few nm) and have a large spectral overlap of donor emission and acceptor absorption spectra.[2,3] Hybrid organic/inorganic semiconductor structures that utilize FRET then offer the prospect of devices that possess a combination of the attractive electrical properties of inorganic materials and the high photoluminescence yields across the visible spectrum that are typical of organic materials.[4] In addition to the resulting technological prospects such structures provide an ideal system to study the interesting, yet experimentally unexplored, nature of nonradiative interactions between inorganic Mott-Wannier (MW) excitons and organic Frenkel excitons.

A prerequisite for energy transfer is that there needs to be a sufficient spectral overlap between the QW emission and the absorption of the organic layer. This favors a choice of QW from the GaN family of alloys since many efficient organic emitters have strong absorption in the blue or ultraviolet spectral range.[4] We have recently reported a temperature-dependent photoluminescence study of hybrid structures comprising thin polyfluorene films (specifically poly[9,9-dioctylfluorene-*co*-9,9-di (4-methoxyphenyl) fluorene] (F8DP)) placed in close proximity to single (Ga,In)N/GaN QWs.[5] This showed that as the separation distance decreased (by reducing the nominal GaN cap layer thickness from ~15 to ~2.5 nm) energy transfer from the QW to the polymer overlayer increased. Here we study the associated nonradiative processes in greater detail using a combination of low-temperature spectrally and temporally resolved optical measurements which show that changes in the flow of energy out of the QW correlate with changes in emission from the polymer layer. Ancillary experiments exclude the possibility that a significant fraction of the energy from the QW is dissipated in nonradiative centers such as surface states or interface defects and we assign the observed behavior to a nonradiative transfer (FRET) process. In addition, we probe the temperature (8–75 K) dependence of the energy transfer process and probe the dipole-dipole character of the nonradiative interaction by analyzing the separation distance dependence of the Förster transfer rates extracted from the luminescence decay curves. Our conclusion is that energy transfer in these structures can be described in terms of efficient resonant Förster coupling between the inorganic MW and the organic Frenkel excitons and that the process is best characterized as a plane-plane interaction.

II. EXPERIMENT

The choice of materials for the hybrid structures was primarily dictated by the requirement for good spectral overlap between the (Ga,In)N/GaN QW emission and the F8DP film absorption.[5] The hybrid heterostructures consist of a thin (~5 nm thickness) layer of the semiconducting polymer F8DP spin-coated from a 4 mg/ml toluene solution onto an energy donor (Ga,In)N/GaN QW structure. The latter QW structures were grown by metalorganic vapor phase epitaxy (MOVPE) on single-side polished (0001)-oriented sapphire substrates, in consecutive growth runs. They differ only in the thickness of the GaN cap above the QW, which was controlled by the growth period for this final layer. More

details of the QW growth conditions and spectroscopic characterization in the as-grown state can be found in Refs. 6 and 7. However, a few growth parameters pertinent to this study are also provided here for completeness. The QWs were grown after depositing a 1 μm thickness layer of high-temperature (HT) GaN, at a setpoint temperature of 1130 °C. The (Ga,In)N/GaN QWs (nominal thickness 2.5 nm) were grown directly on the surface of the HT-GaN buffer, following a growth interruption to allow cooling to a setpoint temperature of 860 °C. Finally, the GaN cap layer was grown at the same temperature as the QW growth, without further interruptions. The target cap layer thicknesses of the three samples used in this study, henceforth designated samples A, B, and C, were, respectively, 15, 4, and 2.5 nm, based on previous growth rate calibrations.

Rutherford backscattering (RBS) measurements were used to determine the GaN cap layer thicknesses of the three samples using a 0.2×0.6 mm^2, collimated beam of 2.0 MeV ^{4}He$^+$ ions (current $\approx$5 nA) with the same experimental configuration described in Ref. 8. RBS data were analyzed with the IBA DATAFURNACE NDF code.[9] The theoretical models and overall methodology used to simulate the RBS spectra have been previously described.[9,10] Atomic force microscopy (AFM) measurements were performed with a commercial MultiMode scanning probe microscope (MultiMode Nanoscope IIIA, Digital Instruments). Surface imaging was performed in a non-contact, tapping mode (resonance frequency 190 kHz) at a scanning speed 1–5 μm/s. Ultrasharp tips, with a radius of curvature $\sim$2 nm were used (cf. standard tips with 5–10 nm).

Samples were optically excited at close to normal incidence using either a *Q*-switched Nd:YAG laser pumped type-II BBO Optical Parametric Oscillator (10 ns pulses, 10 Hz at 360 nm) or the frequency-doubled output of a mode-locked Ti:sapphire laser (150 fs, 76 MHz). The photoluminescence (PL) was spectrally and temporally resolved using a charge coupled device (CCD) and a streak camera (25 ps resolution), respectively. Measurements presented here were obtained from samples held at a temperature in the 8–75 K range using a liquid helium optical cryostat.

III. RESULTS AND DISCUSSION

A. Structural characterization

Any investigation of the Förster interaction processes in a hybrid structure will be dependent on the precision of the growth parameters that control the thickness and morphology of the spacer layer. In our case GaN growth rates can be measured *in situ*, using optical reflectometry[6] but on much thicker layers than those used here. Nominal cap (and QW) thicknesses were inferred from the duration of growth using previous calibrations but in addition the three as-grown samples were carefully analyzed using grazing-incidence RBS to make direct measurements of the GaN cap thicknesses. Conventional RBS is a well-established technique to depth profile the elemental composition of thin films; layer thicknesses and compositions can be determined nondestructively, independent of the effects of strain, and without the use of external standards. The standard depth resolution

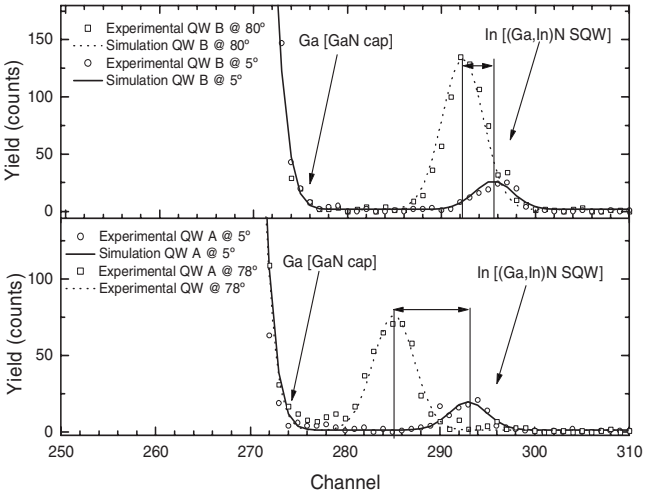

FIG. 1. Measured and simulated RBS spectra from samples A (lower panel) and B (top panel) at near-normal and grazing incidence. The vertical lines through the maxima of the indium scattering peaks emphasize the shift in peak position as the angle of incidence changes.

achieved with RBS is only around 5–10 nm, which is not sufficient to study the single QW heterostructures of interest here. However, depth resolution can be improved markedly if the sample is tilted by a large angle θ, relative to the incoming beam. This translates into an increase of the path length ($\propto 1/\cos\theta$) required to reach a given depth. As a consequence, the scattered particle energy loss increases for a given depth difference. Therefore optimization of the scattering geometry offers a simple and powerful approach to reach the depth resolution necessary to study our (Ga,In)N/GaN single QWs in detail.

Figure 1 shows RBS spectra for two of the samples analyzed, with nominal GaN cap thicknesses of 4 and 15 nm (QW samples B and A, respectively). For clarity, only two spectra at different tilt angles, corresponding to near-normal and glancing incidence, are shown for each sample. In spectra acquired at different tilt angles, the high-energy rising edges of peaks related to chemical elements at the surface maintain the same energy position (corresponding to channel number in the figure). This is evidently the case for the gallium-related backscattering edge, rising off-scale at low channel number in each of the spectra. However, the indium-related peak shifts towards lower energies as the incidence angle increases, because the *effective* thickness of the GaN cap increases with tilt angle. This effect is clearly more pronounced for the sample with the larger cap thickness, a consequence of the greater energy loss experienced by the He$^+$ ions in crossing the thicker GaN cap layer. The experimental RBS spectra at various tilt angles were fitted with the same multilayer model: The most self-consistent analysis was achieved for a common QW composition $Ga_{0.93}In_{0.07}N$ and with GaN cap layer thicknesses $\sim$0.79 times the nominal growth values. This analysis leads to the most probable cap thicknesses, and uncertainty estimates, summarized in Table I. It should be noted that the RBS technique provides information on thicknesses and compositions averaged over the macroscopic beam area. In this regard, these cap thickness

TABLE I. Cap layer thicknesses (and uncertainties) determined from grazing-incidence RBS. The final column lists the rms roughness values (determined by AFM) which show an increase with cap thickness.

Sample designation	RBS most probable cap layer thickness (nm)	RBS cap layer thickness uncertainty (nm)	AFM rms surface roughness (nm)
A	11.8	±0.8	1.1
B	3.2	±0.5	0.6
C	1.9	±0.5	0.3

measurements are more appropriate for our study than the highly localized measurements that can be obtained from cross-sectional transmission electron microscopy.

Good surface morphology of the cap layers is also crucial to our experiments since the polymer overlayer in the hybrid structures is rather thin (<10 nm). The high-temperature GaN buffer layers on which the QWs were grown exhibit a morphology typical of MOVPE growth, comprising atomically flat terraces separated by GaN monolayer steps of height ~0.26 nm.[11] AFM images obtained from sample C with the thinnest cap are shown in Fig. 2 and show terraced surfaces, consistent with a step-flow growth mode.[12] The morphology generally resembles that of the single QWs discussed in Ref. 12, although sample A, with the largest cap thickness, shows rather more curvature of the terrace edges than the other two samples. All three samples show evidence of pits, assumed to be linked to threading dislocations. Similar features on the surface of single QWs were reported in Ref. 12, and were shown to represent an early stage in the evolution of hexagonal V pits which typify thicker (Ga,In)N/GaN multiple QW structures and epilayers.[10,12] The areal density of pits in structure C is 2.4×10^9 cm^{-2}, comparable with the estimated total density of threading dislocations in the GaN buffer layer, while the pit density is a factor of ~3 lower for structures A and B. The pits and steps at terrace edges contribute to the overall root mean square (rms) surface roughness which increases with the cap layer thickness (see Table I). Nevertheless the AFM data suggest reasonably uniform QW and cap layer thicknesses across the terraces and this is supported by x-ray diffraction studies on sample B which showed extensive finite-thickness fringe structure[13] in the vicinity of the GaN (0004) Bragg reflection.

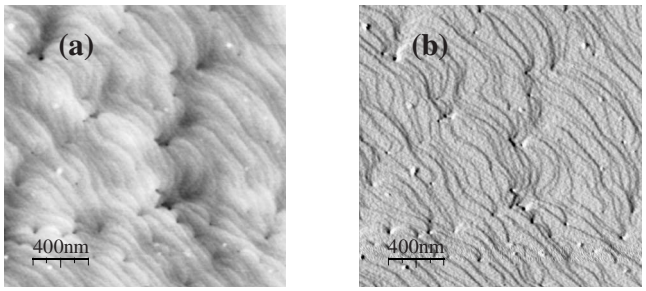

FIG. 2. Height-scaled AFM image (a) and deflection-scaled AFM image (b) of as-grown sample C, illustrating the morphology of the GaN cap. The full tone range corresponds to a height difference of 3 nm.

B. Optical characterization

Figure 3 shows the PL emission spectra obtained from samples A, B, and C at a temperature of 77 K under the same excitation conditions showing that the integrated emission intensities from all three samples are comparable. The differences in the QW emission wavelengths are within the range expected due to variations in well composition and thickness for such narrow InGaN QWs. Figure 4 shows the low temperature PL spectra obtained from the hybrid structures. These spectra can be deconvolved into contributions from the QWs around 385 nm and the polymer at 425 and 455 nm. The most striking aspect of these spectra is the decrease in the relative QW PL intensity and the simultaneous increase in polymer PL emission with decreasing cap thickness. Similar cap-dependent variations in the relative intensities of the QW and polymer emission were seen in spectra obtained from the hybrid structures across the whole 8–75 K temperature range studied. These data provide clear evidence for nonradiative energy transfer from the QW to the polymer. Any radiative energy transfer would be expected to be independent of cap thickness and should not lead to a modification of the donor (QW) emission intensity. We also note that charge, and in particular electron, transfer from the (Ga,In)N QW to the polymer layer is expected to be strongly inhibited by the large energy offset at the GaN/F8DP interface that results in a barrier of the order of 1.5 eV.[14,15] Enhancement of the polymer PL emission due to any unidentified effects

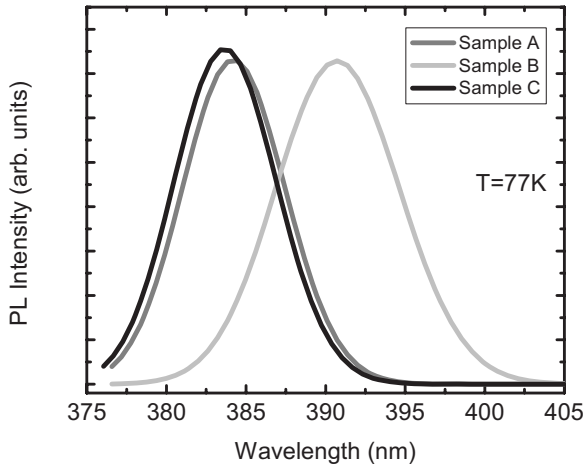

FIG. 3. Low temperature PL spectra obtained from all three QW samples with nominally equal thickness and composition. Note that the integrated intensities are similar.

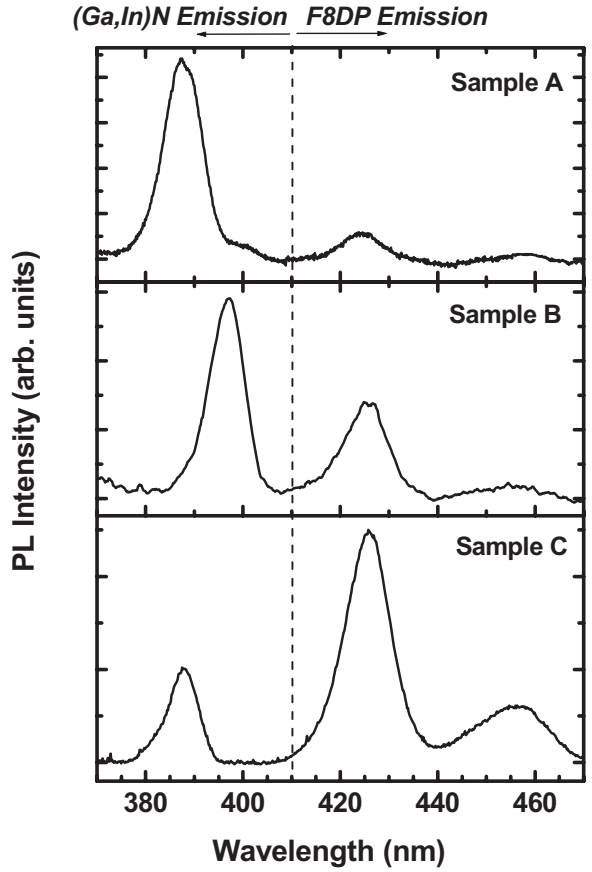

FIG. 4. Low temperature PL spectra obtained from the hybrid structures. With decreasing cap thickness the QW emission decreases while the polymer emission increases consistent with nonradiative energy transfer.

occurring at the GaN/F8DP interface has been previously ruled out by appropriate control experiments.[5]

The efficiency of the energy transfer process can be obtained from time-resolved spectroscopy of the hybrid structures. Initially, our study focuses on an investigation of the QW dynamics to characterize the process of energy out-flow from the QWs. Figure 5 shows QW PL decay curves at $T=15$ K without (black symbols) and with (gray symbols) the F8DP overlayer. It is expected that the PL decays will be characterized by a distribution of lifetimes due to the presence of energetic and spatial disorder in the (Ga,In)N QWs. However, for the purpose of the present discussion, double exponential fits were found to provide a sufficiently good description of the QW decay dynamics. The decays are characterized by a short time constant τ_1 and a much longer time constant τ_2. All decay fits yielded similar τ_1 values of the order of 25 ± 5 ps which we attribute to a spectral overlap of the laser pulse tail with the quantum well emission at early times and this defines the resolution of our system.

The longer time constant τ_2 that characterizes the decay of the QW excitations in the absence of the polymer layer can be expressed as

$$1/\tau_2 = 1/\tau_{\text{radiative}} + 1/\tau_{\text{nonradiative}} \quad (1)$$

and for QWs in the presence of the F8DP overlayer as

$$1/\tau_2 = 1/\tau_{\text{radiative}} + 1/\tau_{\text{nonradiative}} + 1/\tau_{\text{transfer}}. \quad (2)$$

Here $\tau_{\text{radiative}}$ and $\tau_{\text{nonradiative}}$ are the respective radiative and nonradiative lifetimes in the QWs in the absence of energy transfer processes and τ_{transfer} is the characteristic time of the transfer process. The decay fits yield recombination lifetimes $\tau_2=0.91$, 0.72, and 0.77 ns for the QW samples A, B, and C, respectively, with the variation across a sample typically of order ±25 ps. Recombination lifetimes in the 0.6 to 0.9 ns range have been reported previously for similar single (Ga,In)N/GaN wells[16] at low temperature and were attributed to exciton recombination processes in the wells. The variation in lifetime may indicate some influence of surface recombination in the samples having the thinner cap but may also reflect sample-to-sample variations in well composition and thickness.

In contrast, the lifetimes measured for the hybrid structures show a monotonic decrease with decreasing cap thickness with $\tau_2 \approx 0.79$, 0.46, and 0.44 ± 0.025 ns (i.e., $\Delta\tau_2=0.12$, 0.26, and 0.33 ns) for samples A, B, and C, respectively. Quenching of the QW lifetime confirms the presence of an additional nonradiative decay channel that we have previously assigned to FRET.[5] The corresponding Förster energy transfer rate, k_F, can then be determined from $k_F=k_{\text{hybrid}}-k_{\text{QW}}$, where k_{hybrid} and k_{QW} are the (Ga,In)N/GaN QW energy donor PL decay rates (τ_2^{-1}) with and without the F8DP overlayer. Note that k_{QW} depends on both radiative and nonradiative recombination even in the absence of the overlayer. Using the deduced values of k_F and k_{QW} at 15 K leads to FRET efficiencies $\Phi=\{k_F/(k_F+k_{\text{QW}})\}=13.4\pm1.1$, 36.4 ± 2.9, and 42.8 ± 3.4 % for samples A, B, and C, respectively.

We have also investigated the temperature dependence of the FRET efficiency of the thinnest cap structure (sample C) across the 8–75 K range. The results of this study are shown in Fig. 6 where, despite some scatter in the data, there is a clear upward trend in efficiency with increasing temperature. Above 25 K the efficiency exceeds 50% indicating that the majority of QW excitations decay via the FRET channel. Spectrally resolved data presented in Ref. 5 suggests that even greater FRET efficiencies can be expected at higher sample temperatures. However, extending the time-resolved measurements to higher temperatures is not possible due to a significant reduction in the QW PL intensity at temperatures above 75 K. This reduction is attributed to enhanced nonradiative processes that typically dominate recombination in nitride QWs at elevated temperatures as well as the enhanced transfer rates from the QW to the polymer that effectively quench the well emission intensity. Higher laser excitation densities could be used to improve the signal to noise ratio but care needs to be taken to protect the polymer layer from photo-oxidation.

A similar trend for the FRET efficiency with temperature was theoretically predicted for energy transfer from a (Ga,In)N QW to a colloidal quantum dot overlayer[17] and attributed to a temperature-dependent competition between the transfer rate and the radiative rate in the (Ga,In)N QWs. According to Ref. 17, the radiative recombination rate was calculated to reduce faster with temperature than the Förster

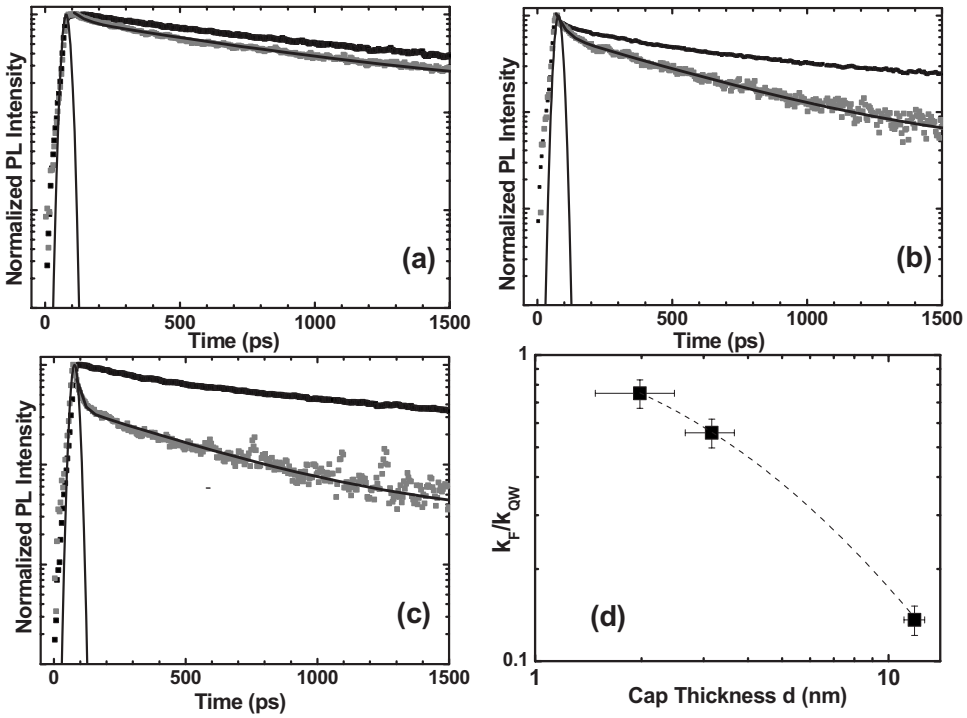

FIG. 5. Comparison of the (normalized) PL decay curves detected at the QW peak with (gray points) and without (black points) the F8DP overlayer for (a) sample A, (b) B, and (c) C. The black solid lines correspond to the biexponential fitting curves and the excitation laser pulse. (d) The dependence of the normalized Förster rate (k_F/k_{QW}) on the measured cap thickness d together with a quadratic fit [using Eq. (4) with $P=2$].

transfer rate so that the transfer rate becomes increasingly effective as the temperature is raised. Additionally, the energy transfer rates could depend on the degree of localization of the donor (QW) excitations. A direct correlation between exciton localization length and FRET rate is theoretically predicted[18] and has been reported to occur for a conjugated polymer guest-host system that supports dipole-dipole transfer.[19]

The radiative transfer efficiency Φ_R is given by

$$\Phi_R \approx Q_{QW} P_{F8DP}, \tag{3}$$

where Q_{QW} is the internal quantum efficiency for emission from the QW and P_{F8DP} is the probability that the QW emission is absorbed by the F8DP overlayer. The latter depends on the absorption coefficient at the QW emission wavelength and the film thickness. Using a value of 3×10^5 cm^{-1} for the F8DP absorption coefficient at 390 nm (Ref. 20) and taking into account Fresnel reflection at the GaN/F8DP interface ($\sim$5% using refractive indices $n_{F8DP}=1.7$ and $n_{GaN}=2.7$ at 390 nm), we estimate that $P_{F8DP}\approx 6.5\%$ assuming that the well emission is isotropic. On the other hand, the (Ga,In)N QW internal quantum efficiency is strongly temperature dependent, ranging from values approaching 100% at low temperatures to values that are an order of magnitude lower ($\sim$10%) at room temperature. Our estimates of the FRET transfer efficiencies are then an order of magnitude larger than Φ_R at low temperature and approximately two orders of magnitude larger at room temperature. FRET therefore appears to be a much more efficient means of energy transfer than radiative pumping, particularly at higher temperatures.

Although FRET is rapid it is nonetheless slow compared with excited state relaxation within the acceptor material (typical relaxation times are in the range of a few hundred fs for polyfluorenes[21]). This ensures that no resonant back-transfer of energy to the donor occurs, a situation referred to as weak coupling. In the strong coupling regime coherent exchange of energy between donor and acceptor is expected to lead to the formation of hybrid exciton states.[22]

In order to study in more detail the nature of the FRET coupling between the (Ga,In)N/GaN QW energy donor and F8DP energy acceptor we have followed the procedure adopted in our earlier investigation of FRET between two different polyfluorene layers separated by a variable thickness inert spacer.[23] The ratio of the FRET and energy donor decay rates, k_F/k_{QW}, is expected to depend on the spacing R between donor and acceptor according to

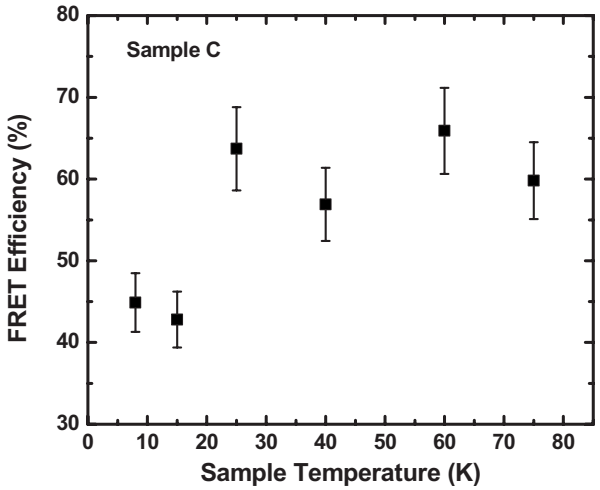

FIG. 6. Förster efficiency deduced from the time resolved data of Fig. 4 for sample C (thinnest cap sample) over the 8–75 K range. There is a clear upward trend in efficiency with increasing temperature.

TABLE II. Fitting results of the dependence of the normalized FRET rate on the cap thickness values using Eq. (4).

Model parameters	$P=2$ ($2D$ to $2D$)	$P=4$ ($0D$ to $2D$)	$P=6$ ($0D$ to $0D$)
R_F (nm)	6.1±0.8	16.5±2.1	27.1±3.3
x (nm)	4.8±0.9	15.2±3.1	25.6±5.8

$$k_F/k_{QW} = [R_F/R]^P, \quad (4)$$

where R_F is the Förster radius (spacing for which the rates are equal). Here $R=(d+x)$ with d the GaN cap layer thickness and x an adjustable correction factor (associated with the finite width of the QW and F8DP layers) that, when added to the measured cap thickness, accounts for the average dipole-dipole separation. The appropriate power P depends on the nature of the dipole-dipole interaction with $P=2$ representing layer-to-layer coupling ($2D$ to $2D$), $P=4$ the coupling between a point dipole and a layer ($0D$ to $2D$) and $P=6$ the coupling between two point dipoles ($0D$ to $0D$). The $T=15$ K dependence of k_F/k_{QW} on the GaN cap layer thickness d, is shown in Fig. 4(d). The cap thickness values are those obtained from the grazing-incidence ion backscattering experiments described above. The abscissa and ordinate error bars represent, respectively, the measurement error in the ion beam backscattering experiments, and the variation in the QW decay lifetimes at different locations on each sample (measurements in the absence/presence of the F8DP overlayer were not made at identical locations). The deduced fitting parameters R_F and x, for the three different dipole-dipole geometries are given in Table II. Given the nominal QW thickness of 2.5 nm and the F8DP layer thickness of 5 nm the x values for $P=4$ and 6 are unreasonably large while that for $P=2$, namely, $x=4.8\pm0.9$ nm, is quite plausible. Similarly, the Förster radius for $P=2$, namely, $R_F=6.1\pm0.8$ nm, is comparable with typical Förster radii for polymer-to-polymer and polymer-to-molecule energy transfer [$R_F\sim3-5$ nm (Refs. 23 and 24)]. The R_F values obtained for the $P=4$ and 6 fits are, however, significantly larger. We thus conclude that the energy transfer in our structures is best described by a $P=2$ dependence, indicative of layer-to-layer dipole coupling. We also propose that the weak dependence on R suggests that short-range multipole interactions such as dipole-quadrupole or exchange coupling, do not significantly contribute to the energy transfer in our samples.

It has been implicitly assumed that the nonradiative transfer described above involved MW and Frenkel exciton interactions. The presence of Frenkel excitons in the organic material is unambiguous since their binding energy (>100 meV) is much larger than kT in the 8–75 K range. On the other hand, the nature of the radiative recombination mechanism in (Ga,In)N QWs is still a matter of debate. Even though the MW exciton binding energy in (Ga,In)N QWs [~53 meV (Ref. 17)] is higher than the thermal energy even at room temperature, strong piezoelectric fields due to the hexagonal crystal symmetry and strain could ionize the excitons[25] so that the dominant radiative mechanism is due to band-to-band (bimolecular) recombination. We have performed power-dependent photoluminescence measurements on the bare QWs that show a QW PL intensity that scales linearly with excitation density. This indicates a monomolecular-dominated radiative decay at all temperatures up to 225 K that can be only attributed to excitonic recombination. Additional support for the excitonic nature of the QW excitations is provided by the time-resolved measurements that show decay lifetimes indicative of radiative recombination due to MW excitons.[16]

IV. CONCLUSIONS

In summary, we have demonstrated efficient Förster resonant coupling (FRET) between Mott-Wannier and Frenkel excitons in hybrid structures comprising single (Ga,In)N quantum wells spaced from F8DP polymer overlayers with variable thickness GaN caps. Spectrally and time-resolved data show that nonradiative energy transfer occurs from the QW (decreasing its PL intensity and recombination lifetime) to the polymer layer (increasing its PL intensity). The efficiency of the energy transfer process was characterized across the 8–75 K range and a power-law dependence indicative of a plane-to-plane dipole-dipole coupling of the MW and Frenkel excitons was obtained. A deeper understanding and subsequent optimization of the FRET mechanisms could lead to novel devices that combine the favorable properties of organic semiconductors and GaN materials. Such devices can have applications in solid state lighting where efficient down conversion into the visible is required[4] and hybrid lasers, where electrically driven (Ga,In)N structures can provide FRET-pumping of organic gain media.[5,26–28]

ACKNOWLEDGMENTS

We thank the Sumitomo Chemical Co., Ltd for providing the polymer used in this study and J. Wilson and C. Belton for useful discussions. We acknowledge Research Councils UK (Basic Technology Research Programme) and the Commission of the European Community (HYTEC IHP Network Project) for financial support.

*Present address: Department of Physics, University of Cyprus, P.O. Box 20537, 1678 Nicosia, Cyprus.

[1] T. Förster, Z. Naturforsch. A **4**, 321 (1949).
[2] V. M. Agranovich, G. C. La Rocca, and F. Bassani, JETP Lett. **66**, 748 (1997).
[3] V. M. Agranovich, D. M. Basko, G. C. La Rocca, and F. Bassani, J. Phys.: Condens. Matter **10**, 9369 (1998).
[4] G. Heliotis, P. N. Stavrinou, D. D. C. Bradley, E. Gu, C. Griffin, C. W. Jeon, and M. D. Dawson, Appl. Phys. Lett. **87**, 103505 (2005).
[5] G. Heliotis, G. Itskos, R. Murray, M. D. Dawson, I. M. Watson, and D. D. C. Bradley, Adv. Mater. (Weinheim, Ger.) **18**, 334 (2006).
[6] C. J. Deatcher, C. Liu, S. Pereira, M. Lada, A. G. Cullis, Y. J. Sun, O. Brandt, and I. M. Watson, Semicond. Sci. Technol. **18**, 212 (2003).
[7] L. T. Tan, R. W. Martin, K. P. O'Donnell, and I. M. Watson, Appl. Phys. Lett. **89**, 101910 (2006).
[8] S. Pereira, E. Pereira, E. Alves, N. P. Barradas, K. P. O'Donnell, C. Liu, C. J. Deatcher, and I. M. Watson, Appl. Phys. Lett. **81**, 2950 (2002).
[9] N. P. Barradas, C. Jeynes, and R. P. Webb, Appl. Phys. Lett. **71**, 291 (1997).
[10] N. P. Barradas, E. Alves, S. Pereira, V. V. Shvartsman, A. L. Kholkin, E. Pereira, K. P. O'Donnell, C. Liu, C. J. Deatcher, I. M. Watson, and M. Mayer, Nucl. Instrum. Methods Phys. Res. B **217**, 479 (2004).
[11] B. Heying, E. J. Tarsa, C. R. Elsass, P. Fini, S. P. DenBaars, and J. S. Speck, J. Appl. Phys. **85**, 6470 (1999).
[12] S. M. Ting, J. C. Ramer, D. I. Florescu, V. N. Merai, B. E. Albert, A. Parekh, D. S. Lee, D. Lu, D. V. Christini, L. Liu, and E. A. Armour, J. Appl. Phys. **94**, 1461 (2003).
[13] T. M. Smeeton, M. J. Kappers, J. S. Barnard, M. E. Vickers, and C. J. Humphreys, Phys. Status Solidi B **240**, 297 (2003).
[14] V. Bougrov, M. E. Levinshtein, S. L. Rumyantsev, and A. Zubrilov, *Properties of Advanced Semiconductor Materials GaN, AlN, InN, BN, SiC, SiGe* (John Wiley & Sons, New York, 2001).
[15] S. Janietz, D. D. C. Bradley, M. Grell, C. Giebler, M. Inbasekaran, and E. P. Woo, Appl. Phys. Lett. **73**, 2453 (1998).
[16] E. S. Jeon, V. Kozlov, Y.-K. Song, A. Vertikov, M. Kuball, A. V. Nurmikko, H. Liu, C. Chen, R. S. Kern, C. P. Kuo, and M. G. Craford, Appl. Phys. Lett. **69**, 4194 (1996); C. K. Sun, S. Keller, T. L. Chiu, G. Wang, M. S. Minsky, J. E. Bowers, and S. P. DenBaars, IEEE J. Sel. Top. Quantum Electron. **3**, 1077 (1997).
[17] S. Kos, M. Achermann, V. I. Klimov, and D. L. Smith, Phys. Rev. B **71**, 205309 (2005).
[18] D. Basko, G. C. La Rocca, F. Bassani, and V. M. Agranovich, Eur. Phys. J. B **8**, 353 (1999).
[19] L. M. Herz, C. Silva, A. C. Grimsdale, K. Mullen, and R. T. Phillips, Phys. Rev. B **70**, 165207 (2004).
[20] R. Xia, G. Heliotis, M. Campoy-Quiles, P. N. Stavrinou, D. D. C. Bradley, Doojin Vak, and Dong-Yu Kim, J. Appl. Phys. **98**, 083101 (2005).
[21] M. Ariu, M. Sims, M. D. Rahn, J. Hill, A. M. Fox, D. G. Lidzey, M. Oda, J. Cabanillas-Gonzalez, and D. D. C. Bradley, Phys. Rev. B **67**, 195333 (2003); O. J. Korovyanko and Z. V. Vardeny, Chem. Phys. Lett. **356**, 361 (2002).
[22] D. M. Basko, G. C. La Rocca, F. Bassani, and V. M. Agranovich, Phys. Rev. B **71**, 165330 (2005); D. G. Lidzey, D. D. C. Bradley, A. Armitage, S. Walker, and M. S. Skolnick, Science **288**, 1620 (2000).
[23] J. Hill, S. Y. Heriot, O. Worsfold, T. H. Richardson, A. M. Fox, and D. D. C. Bradley, Phys. Rev. B **69**, 041303(R) (2004).
[24] T. Virgili, D. G. Lidzey, and D. D. C. Bradley, Adv. Mater. (Weinheim, Ger.) **12**, 58 (2000).
[25] C.-K. Sun, T.-L. Chiu, S. Keller, G. Wang, M. S. Minsky, S. P. Denbaars, and J. E. Bowers, Appl. Phys. Lett. **71**, 425 (1997).
[26] M. Achermann, M. A. Petruska, S. Kos, D. L. Smith, D. D. Koleske, and V. I. Klimov, Nature (London) **429**, 642 (2004).
[27] G. Heliotis, R. Xia, D. D. C. Bradley, G. A. Turnbull, I. D. W. Samuel, P. Andrew, and W. L. Barnes, Appl. Phys. Lett. **83**, 2118 (2003).
[28] M. Campoy-Quiles, G. Heliotis, R. Xia, M. Ariu, M. Pintani, P. Etchegoin, and D. D. C. Bradley, Adv. Funct. Mater. **15**, 925 (2005).